

# REC-RIR: MONAURAL BLIND ROOM IMPULSE RESPONSE IDENTIFICATION VIA DNN-BASED REVERBERANT SPEECH RECONSTRUCTION IN STFT DOMAIN

Pengyu Wang<sup>1,2</sup>      Xiaofei Li<sup>2,3,\*</sup>

<sup>1</sup>Zhejiang University, Hangzhou, China

<sup>2</sup>School of Engineering, Westlake University, Hangzhou, China

<sup>3</sup>Institute of Advanced Technology, Westlake Institute for Advanced Study, Hangzhou, China

## ABSTRACT

Room impulse response (RIR) characterizes the complete propagation process of sound in an enclosed space. This paper presents Rec-RIR for monaural blind RIR identification. Rec-RIR is developed based on the convolutive transfer function (CTF) approximation, which models reverberation effect within narrow-band filter banks in the short-time Fourier transform (STFT) domain. Specifically, we propose a deep neural network (DNN) with cross-band and narrow-band blocks to estimate the CTF filter. The DNN is trained through reconstructing the noise-free reverberant speech spectra. This objective enables stable and straightforward supervised training. Subsequently, a pseudo intrusive measurement process is employed to convert the CTF filter estimate into time-domain RIR by simulating a common intrusive RIR measurement procedure. Experimental results demonstrate that Rec-RIR achieves state-of-the-art (SOTA) performance in both RIR identification and acoustic parameter estimation. Open-source codes are available online at <https://github.com/Audio-WestlakeU/Rec-RIR>.

**Index Terms**— System identification, room impulse response, acoustic parameters, convolutive transfer function, deep learning

## 1. INTRODUCTION

Room impulse response (RIR) models the complete propagation process of sound in an enclosure and contains key information of acoustic characteristics. Accurate RIR estimation facilitates a wide range of applications, such as speech enhancement [1], speech recognition [2] and augmented/virtual reality [3]. A common intrusive method for measuring RIR is implemented by playing a known excitation signal and processing the measured recording signal [4]. However, intrusive RIR measurement is expensive and not always practical in real-world applications. In contrast, blind RIR identification has a broader range of applications. It aims to estimate RIRs solely from observed signals (e.g., reverberant speech signals) without known source signals (e.g., clean speech signals) [5, 6, 7].

With the development of deep neural networks (DNNs), the performance of blind RIR identification has improved significantly. Many approaches encode fixed-length reverberant speech in the time domain and use a decoder to obtain fixed-length RIR estimates. S2IR-GAN [2] uses a generative adversarial network (GAN)-based architecture to estimate the RIR up to 0.25 s. The discriminator network is optimized to differentiate the estimated RIR from the ground truth RIR. Estimating RIR in the time domain remains challenging due to its long taps, which typically consist of thousands of samples. In FiNS [8], the RIR is decomposed into three distinct

components: the direct-path impulse, early reflections and decaying filtered noise signals. A time-domain encoder-decoder architecture is employed to learn both the early RIR and the noise filter, which significantly reduces the output dimension, thus alleviating the difficulty of estimating long RIRs. SG-RIR [9] employs a segmental network that generates one segment of the complete RIR each time, with the network architecture shared across all segments. According to the convolutive transfer function (CTF) approximation [10], the reverberation effect can be modeled within narrow-band filter banks in the short-time Fourier transform (STFT) domain. Therefore, the estimation of long RIR can be replaced by estimating a much shorter CTF filter in the STFT domain, thus simplifying the task. In the STFT domain, BUDDy [11] and VINP [12] estimate RIRs by implicitly reconstructing the reverberant spectra. Neither of them directly estimates the filter through DNN. Instead, since BUDDy and VINP have additional tasks besides RIR identification, both of them iteratively optimize the estimation of clean speech and the filter in STFT domain based on the signal model and DNN predictions.

This work presents Rec-RIR for monaural blind RIR identification. The basis of Rec-RIR is the CTF approximation, which models the reverberation effect within a CTF filter in the STFT domain. Rec-RIR comprises two main steps: CTF filter estimation and a pseudo intrusive measurement process. Using SpatialNet [13] and its derivative methods [12, 14, 15] as the backbone, we propose an end-to-end DNN consisting of cross-band and narrow-band blocks for CTF estimation. The proposed DNN outputs a fixed-length CTF filter based on the input of arbitrary length, allowing Rec-RIR to make full use of the long input recording. Since RIR is independent of noise, and reverberant speech is the filtered version of clean speech through RIR, we propose to learn the embeddings of reverberant speech and clean speech in the latent space, and use both to estimate the CTF filter. We use the reconstruction error of the reverberant spectrum as the primary objective for supervised training, and incorporate two auxiliary losses to provide guidance for the learning of embeddings. The objective enables stable and straightforward estimation of the CTF filter and, compared with BUDDy and VINP, allows the network to directly estimate the CTF filter without iteration. Further, a pseudo intrusive measurement process is introduced to convert the CTF filter into RIR by simulating a common intrusive RIR measurement procedure, as proposed in [12]. Experimental results demonstrate that Rec-RIR can accurately estimate RIRs. Additionally, it achieves state-of-the-art (SOTA) performance in the estimation of acoustic parameters, including reverberation time (RT60), direct-to-reverberant ratio (DRR), and clarity (C50).

The remainder of this paper is organized as follows: Section 2 formulates the signal model. Section 3 details the proposed Rec-RIR. Experiments and discussions are presented in Section 4. Fi-

\* Corresponding author

nally, Section 5 concludes the entire paper.

## 2. SIGNAL MODEL

In the time domain, the noisy reverberant speech recording  $y(n)$  can be modeled as

$$y(n) = x(n) + w(n) = h(n) * s(n) + w(n), \quad (1)$$

where  $n$  is the sample index,  $x(n)$  and  $w(n)$  denote reverberant speech and additive noise, respectively. Reverberant speech  $x(n)$  can be expressed as the convolution of clean speech  $s(n)$  and RIR  $h(n)$ . For simplicity, we assume that the RIR starts exactly at the sample of the direct-path impulse.

Applying STFT to the time-domain signal model, according to the CTF approximation [10], we have

$$\begin{aligned} Y(f, t) &= X(f, t) + W(f, t) \\ &\approx \sum_{l=0}^{L-1} H_l(f) S(f, t-l) + W(f, t), \end{aligned} \quad (2)$$

where  $f$  and  $t$  are the indices of frequency band and frame, respectively.  $Y(f, t)$ ,  $X(f, t)$ ,  $S(f, t)$  and  $W(f, t)$  are the STFT coefficients of  $y(n)$ ,  $x(n)$ ,  $s(n)$  and  $w(n)$ , respectively.  $H_l(f)$  is the  $l$ th coefficient of the  $L$ -order CTF filter at frequency band  $f$ . For simplicity, we define  $\mathbf{Y}, \mathbf{X}, \mathbf{S}, \mathbf{W} \in \mathbb{C}^{F \times T}$  as the spectra of recording, reverberant speech, clean speech and noise, respectively, and we define  $\mathbf{H} \in \mathbb{C}^{F \times L}$  as the entire CTF filter. Then we have

$$\mathbf{Y} = \mathbf{X} + \mathbf{W} \approx \mathbf{H} \circledast \mathbf{S} + \mathbf{W}, \quad (3)$$

where  $\circledast$  denotes temporal convolution operation along the frame axis. CTF approximation models the reverberation effect within narrow-band filter banks in the STFT domain. Since the approximation error is sufficiently small to be neglected [16, 17], RIR and CTF contain nearly identical information. Thus, we are able to convert the estimation of RIR into the estimation of CTF, thereby reducing the filter length of the solution and simplifying the problem.

## 3. PROPOSED METHOD

Rec-RIR aims to estimate RIRs given the noisy and reverberant speech recordings. Specifically, we propose a DNN to learn the mapping from the input spectrum  $\mathbf{Y}$  to the CTF filter estimate  $\hat{\mathbf{H}}$ . Subsequently, a pseudo intrusive measurement process is introduced to convert the CTF filter estimate  $\hat{\mathbf{H}}$  into RIR estimate  $\hat{h}(n)$ . The workflow of Rec-RIR is illustrated in Fig. 1.

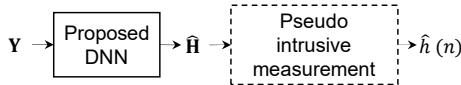


Fig. 1: Workflow of Rec-RIR.

### 3.1. Proposed Network

#### 3.1.1. Feature representation

The input and output features of the proposed DNN are constructed by concatenating the real and imaginary parts of the input spectrum  $\mathbf{Y}$  and CTF filter  $\hat{\mathbf{H}}$  along the expanded channel dimension. The input feature is

$$\mathbf{Y}_{ft} = [\text{Re}\{\mathbf{Y}\}; \text{Im}\{\mathbf{Y}\}] \in \mathbb{R}^{2 \times F \times T}, \quad (4)$$

and the output feature is

$$\hat{\mathbf{H}}_{ft} = [\text{Re}\{\hat{\mathbf{H}}\}; \text{Im}\{\hat{\mathbf{H}}\}] \in \mathbb{R}^{2 \times F \times L}. \quad (5)$$

Similar to  $\mathbf{Y}_{ft}$ , we define  $\hat{\mathbf{X}}_{ft}$  and  $\hat{\mathbf{S}}_{ft}$  as the features of estimated reverberant spectrum and clean spectrum, respectively. The corresponding inverse transformation is straightforward.

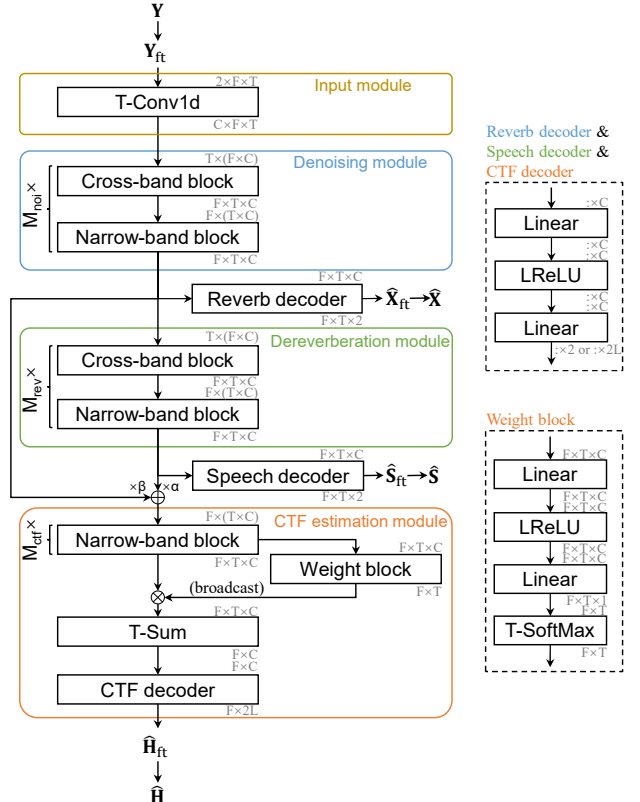


Fig. 2: Architecture of the proposed network.

#### 3.1.2. Modules

As illustrated in Fig. 2, the proposed DNN consists of an input module, a denoising module, a dereverberation module, and a CTF estimation module. The input and output sizes are labeled above and below each block, respectively. For brevity, the reshape and dimension permutation operations are omitted.

**Input module** This module is designed for extracting the embeddings from the noisy and reverberant recording. It consists of a single 1-D convolutional layer applied along the frame axis, with a kernel size of 5 and  $C$  channels, named as T-Conv1d. Through this input module, the 2-channel input features are expanded into  $C$ -dimensional embeddings for each time-frequency (T-F) bin.

**Denoising module and dereverberation module** Since RIR is independent of noise, and reverberant speech is the filtered version of clean speech through RIR, we propose denoising and dereverberation modules to learn the embeddings of reverberant speech and clean speech, respectively. Both modules share the same network structure, which is derived from SpatialNet [13] and oSpatialNet [14] and has been proven effective for denoising and dereverberation tasks. Specifically, the cross-band block, composed of convolutional layers along the frequency axis and linear layers, processes all frames independently using identical model parameters,

and remains consistent with the original design of SpatialNet. In general, RIR identification is an offline task. Therefore, we adopt the bidirectional Mamba-based narrow-band block proposed in [12], which consists of stacked one forward Mamba layer and one backward Mamba layer. The narrow-band block processes all frequency bands independently with the same model parameters. The denoising module and the dereverberation module contain  $M_{\text{noi}}$  and  $M_{\text{rev}}$  stacked cross-band and narrow-band blocks, respectively. Additionally, we employ two decoders that consist of two linear layers and LeakyReLU activation to transform these embeddings into reverberant and clean spectra. Decoders require the output embeddings to contain key information of reverberant and clean speech, providing direct guidance for training.

**CTF estimation module** The outputs of the denoising and dereverberation modules are embeddings containing key information of reverberant and clean speech. The CTF estimation module takes both, and outputs the fixed-length CTF filter estimate. Specifically, the outputs of the denoising and dereverberation modules are weighted and summed to form the input of CTF estimation module with learnable weighting parameters  $\alpha$  and  $\beta$ . According to the CTF approximation, the narrow-band filter banks across different frequency bands are independent. Therefore,  $M_{\text{ctf}}$  stacked narrow-band blocks are employed to estimate CTF embeddings. After that, the weight block, which consists of linear layers, LeakyReLU activation and softmax activation, is designed to calculate the importance of CTF embeddings at all frames. These weights are distinct for each frequency band. Within each band, the sum of weights along the frame axis equals 1. The weighting mechanism ensures a fixed-length output regardless of the input length, allowing Rec-RIR to accept inputs of arbitrary length and make full use of long input recordings. After weighting, we employ a CTF decoder to transform the CTF embeddings into the CTF filter. The CTF decoder shares the same structure as the aforementioned decoders, but differs in that it outputs  $2L$  dimensions for each T-F bin.

### 3.1.3. Loss function

We design a composite loss function for training the proposed network. It comprises three components: the reconstruction error of reverberant spectrum  $\mathcal{L}_{\text{rec}}$ , the prediction error of reverberant spectrum  $\mathcal{L}_{\text{rvb}}$ , and the prediction error of clean spectrum  $\mathcal{L}_{\text{cln}}$ , which is

$$\mathcal{L} = \mathcal{L}_{\text{rec}} + \lambda_{\text{rvb}} \mathcal{L}_{\text{rvb}} + \lambda_{\text{cln}} \mathcal{L}_{\text{cln}}, \quad (6)$$

where  $\mathcal{L}_{\text{rec}} = \mathcal{L}_{\text{RI+Mag}}(\hat{\mathbf{H}} \circledast \mathbf{S}, \mathbf{X})$ ,  $\mathcal{L}_{\text{rvb}} = \mathcal{L}_{\text{RI+Mag}}(\hat{\mathbf{X}}, \mathbf{X})$ ,  $\mathcal{L}_{\text{cln}} = \mathcal{L}_{\text{RI+Mag}}(\hat{\mathbf{S}}, \mathbf{S})$ .  $\lambda_{\text{rvb}}$  and  $\lambda_{\text{cln}}$  are hyperparameters.  $\mathcal{L}_{\text{RI+Mag}}(\cdot, \cdot)$  is defined as [18]

$$\begin{aligned} \mathcal{L}_{\text{RI+Mag}}(\mathbf{X}, \mathbf{Y}) = \frac{1}{FT} & [||\mathbf{X} - \mathbf{Y}||_1 + ||\text{Re}\{\mathbf{X}\} - \text{Re}\{\mathbf{Y}\}||_1 \\ & + ||\text{Im}\{\mathbf{X}\} - \text{Im}\{\mathbf{Y}\}||_1]. \end{aligned} \quad (7)$$

Among these losses,  $\mathcal{L}_{\text{rec}}$  serves as the primary loss, guiding the proposed network to stably learn the direct mapping from the input spectrum to the CTF filter.  $\mathcal{L}_{\text{rvb}}$  and  $\mathcal{L}_{\text{cln}}$  act as auxiliary losses, helping the network obtain better embedding representations.

### 3.2. Pseudo intrusive measurement process

We employ a pseudo intrusive measurement process [12] to convert the CTF filter to RIR by simulating a common intrusive measurement process. Given a logarithmic sine sweep as an excitation signal  $e(n)$ , there is an inverse filter  $v(n)$  that satisfies  $e(n) * v(n) = \delta(n)$ ,

where  $\delta(n)$  is an impulse [4, 19]. Playing such an excitation signal, according to the signal model, the STFT of noise-free measurement signal is

$$\mathbf{Z} \approx \hat{\mathbf{H}} \circledast \mathbf{E}, \quad (8)$$

where  $\mathbf{E}$  is the STFT of excitation signal. The RIR is estimated by inverse filtering

$$\hat{h}(n) = z(n) * v(n), \quad (9)$$

where  $z(n)$  is the inverse STFT of  $\mathbf{Z}$ .

## 4. EXPERIMENTS

### 4.1. Datasets

We focus on audios sampled at 16 kHz. We use the same training and test sets as in VINP [12], which are generated by convolving clean speech with RIRs, followed by noise addition.

For training, the clean speech consists of 200 hours of high-quality utterances from DNS Challenge [20] and VCTK [21], as well as the whole EARS [22] corpus. We use 100,000 reverberant and direct-path RIR pairs simulated by gpuRIR [23], in which the speaker and microphone are randomly placed in rooms with dimensions randomly selected within a range of 3 m to 15 m for length and width, and 2.5 m to 6 m for height. Reverberant RIRs have RT60s uniformly distributed within the range of 0.2 s to 1.5 s. To align the clean speech with the recording, we use the direct-path version of the observed signal as the clean speech in our loss function. Direct-path RIRs are generated using the same geometric parameters as the reverberant ones but with an absorption coefficient of 0.99. Noise comes from NOISEX-92 [24] and the training set of REVERB Challenge [25]. The signal-to-noise ratio (SNR) is uniformly distributed within the range of 5 dB to 20 dB.

We use the SimACE test set proposed in [12], in which the microphone recordings are generated by convolving the clean speech from the 'si\_et\_05' subset in WSJ0 corpus [26] with the downsampled measured RIRs from the 'Single' subset in ACE Challenge [27], and adding noise from the test set in REVERB Challenge with a SNR of 20 dB. The reference minimum and maximum RT60s are 0.332 s and 1.22 s, respectively [27]. During testing, the labels of acoustic parameters are computed from the ground truth RIRs [12].

### 4.2. Settings

Before Rec-RIR, the input recordings are normalized using their maximum absolute value. The STFT analysis and synthesis windows are square-root Hann windows with a length of 512 samples and 50% overlap, which means  $F = 257$ . The numbers of layers in the proposed DNN are  $M_{\text{noi}} = 2$ ,  $M_{\text{rev}} = 6$  and  $M_{\text{ctf}} = 4$ . The dimension of embeddings is set to  $C = 96$ . The CTF length is set to  $L = 60$ , which corresponds to RIR estimates with an effective length of approximately 0.96 s. With the above settings, Rec-RIR has 3.1 M parameters and 62.2 GFlops/s computational complexity.

For training, we set  $\lambda_{\text{rvb}} = 1$  and  $\lambda_{\text{cln}} = 1$ , segment speech utterances into 4 s, and use 97,092 samples per epoch with a batch size of 4. We adopt the AdamW optimizer [28] and the cosine annealing learning rate scheduler with restarts. The learning rate starts at 0.001 per epoch, decays cosinely, and reaches its minimum at the end of epoch. Training runs for 35 epochs total.

In the pseudo intrusive measurement process, we employ the logarithmic sine sweep signal [4, 19] with a frequency range of 62.5 Hz to 8000 Hz and a duration of 8.192 s as the excitation signal. Fade-in with 256 samples and fade-out with 128 samples are applied to mitigate spectral leakage.

**Table 1:** Blind RIR identification results on SimACE.

Method	RIR-50 ms	RT60 (s)			DRR (dB)			C50 (dB)		
	RMSE $\downarrow$	MAE $\downarrow$	RMSE $\downarrow$	$\rho\uparrow$	MAE $\downarrow$	RMSE $\downarrow$	$\rho\uparrow$	MAE $\downarrow$	RMSE $\downarrow$	$\rho\uparrow$
FiNS [8]	0.097	0.113	0.167	0.857	2.153	2.639	0.737	6.489	6.597	0.925
BUDDy (pre-trained) [11]	0.054	0.124	0.173	0.941	3.931	4.570	0.783	4.290	4.654	0.773
BUDDy [11]	0.057	0.122	0.166	0.952	3.673	4.360	0.774	4.109	4.477	0.779
VINP-TCN+SA+S [12]	0.050	0.089	0.124	0.934	3.256	3.764	0.872	0.914	1.135	0.961
VINP-oSpatialNet [12]	0.050	0.103	0.154	0.895	2.398	2.875	0.908	0.977	1.295	0.943
<b>Rec-RIR</b>	<b>0.040</b>	<b>0.069</b>	<b>0.104</b>	<b>0.994</b>	<b>0.684</b>	<b>0.794</b>	<b>0.994</b>	<b>0.858</b>	<b>1.019</b>	<b>0.978</b>

#### 4.3. Comparison methods and metrics

We compare Rec-RIR with FiNS [8], BUDDy [11] and VINP [12]. Part of convolutional kernels in FiNS are modified to handle the 16 kHz inputs. For BUDDy, we additionally provide the results using its official pre-trained weights.

We evaluate Rec-RIR using acoustic parameters RT60, DRR and C50. We present their mean absolute error (MAE), root mean square error (RMSE), and Pearson correlation coefficient ( $\rho$ ). Additionally, we provide the RMSE of early reflections (marked as RIR-50 ms), corresponding to the 50 ms duration after the direct-path impulse.

#### 4.4. Results and analysis

As shown in Table 1, Rec-RIR achieves the SOTA estimation of the early reflections and the acoustic parameters. The Pearson correlation coefficient of Rec-RIR is close to 1, indicating a more stable and consistent estimation compared to other methods. Unlike FiNS which learns the early reflections and the noise shaping filters directly from fixed-length inputs, BUDDy, VINP, and Rec-RIR solve the filter in STFT domain based on the spectra of reverberant recordings with arbitrary length. Among these three approaches, the DNNs in BUDDy and VINP do not directly output the filter coefficients. Instead, they alternately update the estimates of clean speech and filters according to the signal model and derive the final estimates after multiple iterations by maximizing likelihood. Differently, Rec-RIR introduces the DNN and loss functions specifically designed for RIR estimation, enabling a direct estimation of CTF filter without the need for any iteration, thus reducing the computational complexity. Fig. 3 shows an example of the estimated RIR, whose ground truth RT60, DRR and C50 are 1.26 s, -1.24 dB and 4.90 dB, respectively. It can be found that Rec-RIR is capable of estimating the impulses in early reflections. The impulses in the measured RIR that occur before 2 ms cannot be fully reconstructed, which is reasonable because these impulses correspond to the frequency response of the measurement system. During training, we use the direct-path signal as the clean speech to obtain the aligned time delay and gain. However, since the direct-path signal contains the frequency response, the estimated CTF filter may lack the corresponding component. Fig. 4

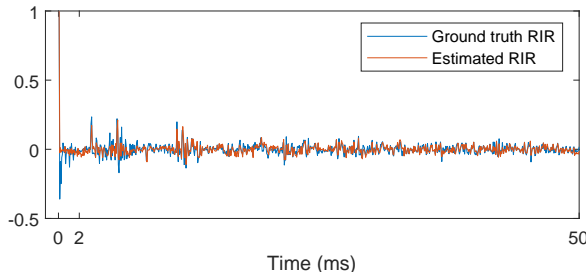


**Fig. 3:** Example of ground truth and estimated RIRs.

presents the 2-D projections of the CTF embeddings (before the CTF decoder), where the inputs are derived from the entire test set and the projections are generated using UMAP [29]. As observed, the embeddings within the latent space exhibit a clear clustering corresponding to the RIR IDs.

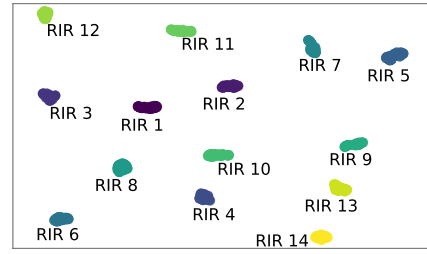


**Fig. 4:** 2-D projections of CTF embeddings on SimACE.

#### 4.5. Ablation study

An ablation study with variant loss weights is designed to demonstrate the contribution of the auxiliary losses. We present the mean values and standard deviations of metrics in Table 2. Compared with Var-1 which estimates the CTF filter directly using the primary loss, other experiments have lower errors, indicating that both auxiliary losses contribute to the final performance. The MAEs of RT60 for Var-2, Var-3 and Rec-RIR are close. We further employ the two-tailed Z-test to analyze their differences. Results show that there are no significant statistical differences in RT60 estimation between Rec-RIR and Var-2 as well as Var-3 with p-values  $p > 0.999$  and  $p \approx 0.306 > 0.05$ , respectively. Therefore, the proposed setting is the best among all evaluated settings.

**Table 2:** Ablation study for loss functions.

Exp. ID	$\lambda_{rvb}$	$\lambda_{cln}$	RT60 (s)	DRR (dB)
			MAE $\downarrow$	MAE $\downarrow$
Var-1	0.0	0.0	0.077 $\pm$ 0.080	1.056 $\pm$ 0.505
Var-2	1.0	0.0	<b>0.069<math>\pm</math>0.074</b>	0.899 $\pm$ 0.582
Var-3	0.0	1.0	<b>0.065<math>\pm</math>0.062</b>	0.960 $\pm$ 0.394
<b>Rec-RIR</b>	<b>1.0</b>	<b>1.0</b>	<b>0.069<math>\pm</math>0.078</b>	<b>0.684<math>\pm</math>0.402</b>

## 5. CONCLUSION

In this work, we propose Rec-RIR for blind RIR identification. According to CTF approximation, we propose an end-to-end DNN that consists of cross-band and narrow-band blocks with auxiliary losses to estimate the CTF filter by reconstructing the reverberant speech spectrum in the STFT domain. A pseudo intrusive measurement process is employed to simulate the common intrusive RIR measurement process and transform the CTF filter into RIR. Experimental results show that Rec-RIR attains SOTA estimation of RIR and acoustic parameters.

## 6. REFERENCES

- [1] E. Vincent, T. Virtanen, and S. Gannot, *Audio source separation and speech enhancement*, John Wiley & Sons, 2018.
- [2] A. Ratnarajah, I. Ananthabhotla, V. Ithapu, et al., “Towards improved room impulse response estimation for speech recognition,” in *ICASSP 2023*. IEEE, 2023, pp. 1–5.
- [3] C. Schissler, R. Mehra, and D. Manocha, “High-order diffraction and diffuse reflections for interactive sound propagation in large environments,” *ACM Transactions on Graphics (TOG)*, vol. 33, no. 4, pp. 1–12, 2014.
- [4] G. Stan, J. Embrechts, and D. Archambeau, “Comparison of different impulse response measurement techniques,” *Journal of the Audio engineering society*, vol. 50, no. 4, pp. 249–262, 2002.
- [5] Y. Lin and D. Lee, “Bayesian regularization and nonnegative deconvolution for room impulse response estimation,” *IEEE Transactions on Signal Processing*, vol. 54, no. 3, pp. 839–847, 2006.
- [6] K. Crammer and D. Lee, “Room impulse response estimation using sparse online prediction and absolute loss,” in *2006 IEEE International Conference on Acoustics Speech and Signal Processing Proceedings*. IEEE, 2006, vol. 3, pp. III–III.
- [7] M. Crocco and A. Del Bue, “Room impulse response estimation by iterative weighted l1-norm,” in *EUSIPCO 2015*. IEEE, 2015, pp. 1895–1899.
- [8] C. Steinmetz, V. Ithapu, and P. Calamia, “Filtered noise shaping for time domain room impulse response estimation from reverberant speech,” in *2021 IEEE Workshop on Applications of Signal Processing to Audio and Acoustics*. IEEE, 2021, pp. 221–225.
- [9] Z. Liao, F. Xiong, J. Luo, et al., “Blind estimation of room impulse response from monaural reverberant speech with segmental generative neural network,” in *Interspeech 2023*, 2023, pp. 2723–2727.
- [10] R. Talmon, I. Cohen, and S. Gannot, “Relative transfer function identification using convolutive transfer function approximation,” *IEEE Transactions on audio, speech, and language processing*, vol. 17, no. 4, pp. 546–555, 2009.
- [11] J. Lemercier, E. Moliner, S. Welker, et al., “Unsupervised blind joint dereverberation and room acoustics estimation with diffusion models,” *IEEE Transactions on Audio, Speech and Language Processing*, vol. 33, pp. 2244–2258, 2025.
- [12] P. Wang, Y. Fang, and X. Li, “Vinp: Variational bayesian inference with neural speech prior for joint asr-effective speech dereverberation and blindrir identification,” *arXiv preprint arXiv:2502.07205*, 2025.
- [13] C. Quan and X. Li, “Spatialnet: Extensively learning spatial information for multichannel joint speech separation, denoising and dereverberation,” *IEEE/ACM Transactions on Audio, Speech, and Language Processing*, vol. 32, pp. 1310–1323, 2024.
- [14] C. Quan and X. Li, “Multichannel long-term streaming neural speech enhancement for static and moving speakers,” *IEEE Signal Processing Letters*, vol. 31, pp. 2295–2299, 2024.
- [15] N. Shao, R. Zhou, P. Wang, et al., “Cleannel: Mel-spectrogram enhancement for improving both speech quality and asr,” *IEEE Transactions on Audio, Speech and Language Processing*, pp. 1–13, 2025.
- [16] Y. Avargel and I. Cohen, “System identification in the short-time fourier transform domain with crossband filtering,” *IEEE transactions on Audio, Speech, and Language processing*, vol. 15, no. 4, pp. 1305–1319, 2007.
- [17] J. Tang, W. Zhu, and X. Li, “Personal sound zones in the short-time fourier transform domain with relaxed reverberation,” *The Journal of the Acoustical Society of America*, vol. 157, no. 2, pp. 778–796, 2025.
- [18] Z. Wang, G. Wichern, and J. Le Roux, “On the compensation between magnitude and phase in speech separation,” *IEEE Signal Processing Letters*, vol. 28, pp. 2018–2022, 2021.
- [19] A. Farina, “Simultaneous measurement of impulse response and distortion with a swept-sine technique,” in *Audio engineering society convention 108*. Audio Engineering Society, 2000.
- [20] C. Reddy, V. Gopal, R. Cutler, et al., “The interspeech 2020 deep noise suppression challenge: Datasets, subjective testing framework, and challenge results,” in *Interspeech 2020*, 2020, pp. 2492–2496.
- [21] C. Valentini-Botinhao, X. Wang, S. Takaki, et al., “Investigating rnn-based speech enhancement methods for noise-robust text-to-speech,” in *SSW 2016*, pp. 146–152.
- [22] J. Richter, Y. Wu, S. Krenn, et al., “EARS: An anechoic full-band speech dataset benchmarked for speech enhancement and dereverberation,” in *Interspeech*, 2024, pp. 4873–4877.
- [23] D. Diaz-Guerra, A. Miguel, and J. Beltran, “gpurir: A python library for room impulse response simulation with gpu acceleration,” *Multimedia Tools and Applications*, vol. 80, no. 4, pp. 5653–5671, 2021.
- [24] A. Varga and H. Steeneken, “Assessment for automatic speech recognition: II. noisex-92: A database and an experiment to study the effect of additive noise on speech recognition systems,” *Speech communication*, vol. 12, no. 3, pp. 247–251, 1993.
- [25] K. Kinoshita, M. Delcroix, T. Yoshioka, et al., “The reverb challenge: A common evaluation framework for dereverberation and recognition of reverberant speech,” in *2013 IEEE Workshop on Applications of Signal Processing to Audio and Acoustics*. IEEE, 2013, pp. 1–4.
- [26] D. Paul and J. Baker, “The design for the wall street journal-based csr corpus,” in *Speech and Natural Language: Proceedings of a Workshop Held at Harriman, New York, February 23-26, 1992*, 1992.
- [27] J. Eaton, N. Gaubitch, A. Moore, et al., “Estimation of room acoustic parameters: The ace challenge,” *IEEE/ACM Transactions on Audio, Speech, and Language Processing*, vol. 24, no. 10, pp. 1681–1693, 2016.
- [28] I. Loshchilov and F. Hutter, “Decoupled weight decay regularization,” in *ICLR*, 2018.
- [29] L. McInnes, J. Healy, N. Saul, et al., “Umap: Uniform manifold approximation and projection,” *The Journal of Open Source Software*, vol. 3, no. 29, pp. 861, 2018.